5-1-1988

Wavelength Dependence of Eddy Dissipation and Coriolis Force in the Dynamics of Gravity Wave Driven Fluctuations in the OH Nightglow

Michael P. Hickey Ph.D.
Embry-Riddle Aeronautical University, hicke0b5@erau.edu

JOURNAL OF GEOPHYSICAL RESEARCH, VOL. 93, NO. A5, PAGES 4089–4101, MAY 1, 1988

Wavelength Dependence of Eddy Dissipation and Coriolis Force in the Dynamics of Gravity Wave Driven Fluctuations in the OH Nightglow

M. P. HICKEY

Universities Space Research Association, NASA Marshall Space Flight Center, Huntsville, Alabama

The theory of Walterscheid et al. (1987) to explain internal gravity wave induced oscillations in the emission intensity I and rotational temperature T of the OH nightglow was modified by Hickey (1988) to include the effects of eddy dissipation and Coriolis force. In the theory of Walterscheid et al. (1987) the ratio $\eta = (\delta I/I_0)/(\delta T/T_0)$ (δ refers to a perturbation quantity, and a zero subscript refers to an average) was found to be independent of horizontal wavelength at long periods, while in the extended theory of Hickey (1988) some such dependence was inferred. In the present paper the horizontal wavelength dependence of η is examined. It is found that values of η will be dependent on both wave period and horizontal wavelength, meaning that in order to compare measurement with theory, horizontal wavelengths will need to be measured in conjunction with the OH nightglow measurements. At long periods the modifications to η by the inclusion of eddy dissipation are much larger for the shorter horizontal wavelength waves, although such modifications may be more observable for some of the longer horizontal wavelength waves. The Coriolis force is important only for waves of very large horizontal wavelength.

INTRODUCTION

In order to describe wave-driven fluctuations in the OH nightglow, *Walterscheid et al.* [1987] have devised a comprehensive model which incorporates a five-reaction photochemical scheme and the Eulerian dynamics of linearized acoustic-gravity waves in an isothermal, motionless, and dissipationless atmosphere. They found that *Krassovsky's* [1972] ratio η $(=(\delta I/I_0)/\delta T/T_0)$, where I is the nightglow intensity, T is the rotational temperature, a zero subscript refers to an undisturbed quantity, and a δ refers to the wave-associated quantity) is a complex quantity which depends sensitively on the altitude of the OH emission layer (z_{OH}) as well as on the wave period and the atomic oxygen scale height (H(O)). At gravity wave periods of hours, η was found to be virtually independent of horizontal wavelength (λ_x), although some such dependence was found for the waves close to their regions of evanescence (i.e., for the waves having high horizontal phase-trace speeds). This model was then used by *Hecht et al.* [1987] and *Sivjee et al.* [1987] in order to compare observations made of the OH nightglow at a single observing site with theory. The plausibility of the association of the observations with theory was established, and it was found that in order to obtain best agreement between the two it was sometimes necessary to experiment with the values of z_{OH} and H(O) used in the model.

Hickey [1988] modified this model by including both eddy viscosity and eddy thermal conduction as well as (by employing the "shallow atmosphere" approximation) the Coriolis force in the gravity wave dynamics (the acoustic waves were not treated in that study). For the same nominal case as studied by *Walterscheid et al.* [1987] (i.e., $\lambda_x = 100$ km, $z_{OH} = 83$ km, $H(O) = -2.8$ km), it was found that the Coriolis force was unimportant at any wave period, and when included by itself, so too was the eddy viscosity. However, the effect of the eddy thermal conduction on η was very pronounced for wave periods of a couple of hours or more, while this effect was reduced (though not to any level of insignificance) with the further inclusion of the eddy viscosity. For wave periods of a couple of hours or more the effect of the inclusion of eddy dissipation was to increase (dramatically so for the longest of wave periods) the magnitude of η and to decrease the phase of η.

However, *Hickey* [1988] demonstrated that the longer-period waves were experiencing a dissipation severe enough to be causing their wave amplitudes to be decreasing with increasing altitude and that they would have therefore presumably reached their maximum amplitude at lower altitudes. Thus these waves would have had diminished amplitudes and, like their associated values of η, would not have been as easily observable as they may otherwise have been in the absence of any dissipation. The short-period waves were found to be experiencing little dissipation, so that their wave amplitudes would still have been increasing with increasing altitude, and, not yet having achieved their maximum amplitudes, they would not have been as observable as they may otherwise have been. At intermediate periods the waves were found to be experiencing a zero (or close to zero) amplitude growth as a consequence of the dissipation just offsetting the natural amplitude growth which would normally occur with increasing altitude in the absence of any dissipation. Thus it was concluded that these waves would be achieving their maximum amplitudes and hence, source generation and nonlinear or saturation effects aside, would be more observable than either the short-period or the long-period waves. In view of the dependence of η on wave period it was also concluded that while very large modifications to the values of η would rarely be observed, at times a close agreement between observation and theory would require the inclusion of dissipation in the modeling of the gravity wave dynamics.

It was also indicated by *Hickey* [1988] that η would depend sensitively on λ_x, since the thermal conduction parameter appearing in the dynamical factors is proportional to λ_x^{-2}. This is in contrast to the results of the calculations of *Walterscheid et al.* [1987] which did not include dissipation, where it was

Paper number 7A9293.
0148-0227/88/007A-9293$05.00

found that η was virtually independent of λ_x at gravity wave periods of hours. Hence it was concluded that one could not a priori preclude the effects of dissipation without first having some estimate of the horizontal wavelength, which in turn questioned some of the comparisons which have been made between observations made at a single observing site with the dissipationless theory.

In the present paper, results obtained from the model of *Walterscheid et al.* [1987] are compared with those obtained using the modifications to this model as described by *Hickey* [1988]. The results are divided into two parts. In the first part the effects of Coriolis force are not included, and results are presented for horizontal wavelengths of 10, 100, 1000, and 10,000 km so that the dependence of η on horizontal wavelength can be examined. In the second part the Coriolis force is included both with and without the inclusion of eddy dissipation and for horizontal wavelengths of 1000 and 10,000 km.

THEORY

The basic theory and underlying assumptions used in the model have been described in detail by *Walterscheid et al.* [1987], while the extension of the theory to include the effects of eddy viscosity, eddy thermal conduction, and Coriolis force in the gravity wave dynamics has been described by *Hickey* [1988]. Because of this, only a general description of the model will be provided here, and the reader is referred to these previous papers for a more detailed description. However, the appendix contains some of the gravity wave equations used in the present paper, while the approximations used in deriving such equations are discussed in detail by *Hickey and Cole* [1987].

Basically, the model incorporates a five-reaction photochemical scheme (involving the minor species OH, O_3, H, O, and HO_2) in order to describe the production and loss of OH. Molecular oxygen and nitrogen compose the background major gas, and the molecular oxygen is assumed to have a constant mixing ratio with respect to the major gas. For each of the minor species a linearized continuity equation is written involving chemical production and loss terms which themselves involve wave-imparted density fluctuations of the major gas, an advection term due to the wave-imparted vertical velocity, and a compressional term due to the wave-imparted velocity divergence. All species have the same temperature T and velocity v as the background major gas. The velocity divergence, the vertical velocity, and the major gas density perturbation are each related to the temperature perturbation through dynamical factors designated f_1, f_2, and f_3, respectively. These three dynamical factors were calculated by *Walterscheid et al.* [1987] employing the most basic gravity wave theory as given by *Hines* [1960]. However, *Hickey* [1988] modified these dynamical factors to include the effects of eddy viscosity, eddy thermal conduction, and the Coriolis force, and these are provided in the appendix following the notation of *Hickey and Cole* [1987]. With this done, the system of five continuity equations describing the density perturbations for each of the five minor species is written in terms of the relative temperature perturbation from which, given a relative temperature perturbation, solutions are obtained using standard matrix inversion techniques. Results are normalized with respect to the relative temperature perturbation and, using the nightside model atmosphere of *Winick* [1983], the density perturbations of the minor species are calculated. From this, so too is Krassovsky's ratio η, using equation (14) of *Walterscheid et al.* [1987].

RESULTS

Dependence on Horizontal Wavelength

In this section of results the dependence of η on horizontal wavelength is examined without the inclusion of the Coriolis force. Results are displayed for horizontal wavelengths of 10, 100, 1000, and 10,000 km and for a broad range of wave periods corresponding to internal gravity waves. For each particular wavelength the results will cover a different period range because the region of evanescence extends to greater periods for the longer-wavelength waves because the horizontal phase trace speed of internal gravity waves is necessarily less than about 0.9 times the local sound speed. Dissipation is due to both eddy viscosity and eddy thermal conduction, the values of the eddy coefficients being taken from *Hickey* [1988]. Results will be displayed only for the imaginary parts of the vertical wave numbers and for the magnitudes and phases of η and the dynamical factors f_1, f_2, and f_3. Amplitudes and phases of the fluctuations of the various minor species will not be shown here but will appear in a NASA contract report which is currently in preparation.

Figure 1 shows the imaginary part of the vertical wave number (Im (k_z)) for each of the horizontal wavelengths as a function of wave period. Also shown is the value of $1/2H$, where H is the pressure scale height. For each of the Im (k_z) curves in this figure an intersection with the $1/2H$ line corresponds to those waves which are experiencing a zero amplitude growth because the amplitudes of gravity waves have an altitude (z) dependence of the form exp $[1/2H + \text{Im}\ (k_z)]z$. In the absence of any dissipation, Im $(k_z) = 0$ and the wave amplitudes grow with increasing altitude as exp $[z/2H]$. To the left of such points of intersection (i.e., at shorter periods) the waves are experiencing less dissipation and are thus still growing with increasing altitude $(1/2H + \text{Im}\ (k_z) > 0)$ and will continue to do so until, at higher altitudes where the dissipation rates have presumably increased sufficiently, they reach their maximum amplitudes. To the right of these points of intersection (at longer periods) the waves are experiencing severe dissipation, the wave amplitudes are decreasing with increasing altitude $(1/2H + \text{Im}\ (k_z) < 0)$, and these waves must therefore have already reached their maximum amplitudes at lower altitudes where the dissipation rates are (presumably) smaller. The results from this figure are very important as far as the results for the rest of this section are concerned because they indicate how observable some of the effects considered here may be. Usually, one would expect to observe (source generation and nonlinear or saturation effects aside) those waves achieving, or close to achieving, their maximum amplitudes, which in this figure occurs where an Im (k_z) line intersects the $1/2H$ line. Therefore, on most of the following figures, arrows will be used to show at what periods, for each of the horizontal wavelengths, maximum amplitudes (or zero amplitude growths) occur. One notices from this figure that the point of zero amplitude growth occurs at longer wave periods for the longer-wavelength waves and that at a given wave period the longer-wavelength waves are experiencing less dissipation than the shorter-wavelength waves.

The magnitude of the dynamical factor f_1 is shown in Figure 2*a*. In the absence of dissipation, $|f_1|$ is independent of horizontal wavelength and, though not shown, would be represented as a straight line connecting the points labeled A and B. With dissipation included, $|f_1|$ is wavelength dependent, which is especially noticeable at the longer wave periods. As the horizontal wavelength is increased, $|f_1|$ follows more close-

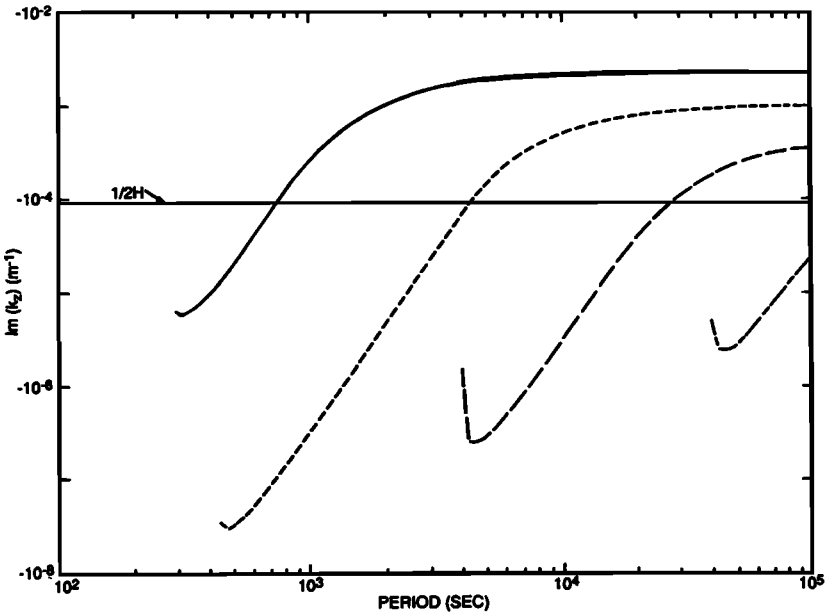

Fig. 1. Imaginary part of the vertical wave number (k_z) versus period calculated with eddy dissipation and without Coriolis force for horizontal wavelengths of 10 km (solid curve), 100 km (short-dashed curve), 1000 km (long-dashed curve), and 10,000 km (short-and-long-dashed curve). Without dissipation, Im (k_z) = 0. The solid horizontal line shows the value of 1/2H.

ly its dissipationless value. This is most noticeable for the 10,000-km wavelength wave, which, experiencing little dissipation, has $|f_1|$ decreasing linearly with increasing period. For each value of horizontal wavelength the dependence of $|f_1|$ on period departs from an inverse linear one (i.e., from the nondissipative dependence) at periods close to where the waves are reaching their maximum amplitudes, as indicated by the arrows. For the shorter-wavelength waves, $|f_1|$ becomes almost constant and independent of period at long periods and is significantly larger than its nondissipative value.

The phase of f_1 is shown in Figure 2*b*. In the absence of any dissipation, f_1 is purely imaginary and equal to $-i\omega/(\gamma - 1)$ (ω is the wave angular frequency, and γ is the usual ratio of specific heats), so that its phase is a constant equal to $-90°$. With the inclusion of dissipation the phase of f_1 is no longer constant, although it approaches a constant value (very close to $-120°$) at long periods for the short horizontal wavelength waves. One notices that at periods where the waves are achieving their maximum amplitudes the phases of f_1 depart from their dissipationless values by an increasing amount as the horizontal wavelengths increase, as indicated by the arrows.

The magnitude of f_2 is shown in Figure 3*a*. Apart from the 10-km wavelength wave, $|f_2|$ displays a nonlinear dependence on wave period for periods close to the regions of evanescence (i.e., at the extreme left-hand parts of the individual curves), which is the same result obtained in the absence of dissipation. At slightly greater periods, $|f_2|$ decreases linearly with increasing period both with and without the inclusion of dissipation. In the absence of dissipation, $|f_2|$ would remain independent of horizontal wavelength and would continue to decrease linearly with increasing period. However, with dissipation included, $|f_2|$ approaches a wavelength-dependent constant value at the long wave periods for the shorter horizontal wavelengths, which is significantly greater than its dissipationless value and which is larger for the shorter-wavelength waves. The value of $|f_2|$ for the 10,000-km wavelength wave is virtually unchanged by the inclusion of dissipation as a consequence of the low dissipation rates associated with this value of wavelength.

The phase of f_2 is shown in Figure 3*b* both with and without the inclusion of dissipation. At the shortest of wave periods for each particular wavelength the phase of f_2 calculated with dissipation is equal to that calculated without dissipation, but as the period is increased, this is no longer true. At the periods where the maximum amplitudes are occurring the two are noticeably different, with the biggest differences occurring for the longer-wavelength waves. With the inclusion of dissipation the phase of f_2 approaches a constant value of about $-120°$ at long periods for the shorter-wavelength waves, but without it this value is closer to $-90°$.

The magnitude of f_3 calculated with the inclusion of dissipation is shown in Figure 4*a*. For both the 10- and the 100-km wavelength waves $|f_3|$ is unaffected by the inclusion of dissipation at short periods, but whereas without the inclusion of dissipation it approaches a value of unity at long periods, with its inclusion it approaches a value slightly greater than unity. With the inclusion of dissipation, $|f_3|$ never deviates by more than 10% from its dissipationless value for the 1000- and 10,000-km wavelength waves. It is apparent that the effect of dissipation on $|f_3|$ is not as pronounced as it is upon both $|f_1|$ and $|f_2|$.

The phase of f_3 is shown in Figure 4*b*. Again, dissipation is not as severe here as it is for the phases of f_1 and f_2. The effect of the inclusion of dissipation is to slightly decrease the magnitude of the phase of f_3 at long periods, the effect being greater for the shorter-wavelength waves.

The magnitudes of η for the four values of horizontal wavelength and with dissipation included are shown in Figure 5*a*. Also shown is the value of $|\eta|$ calculated without dissipation for the 10-km wavelength wave. The value of $|\eta|$ is virtually unaffected by the inclusion of dissipation at any period for the 10,000-km wavelength wave. For the 10-, 100-, and 1000-km wavelength waves, $|\eta|$ is unaffected by the inclusion of dissipation at short wave periods close to each of the respective

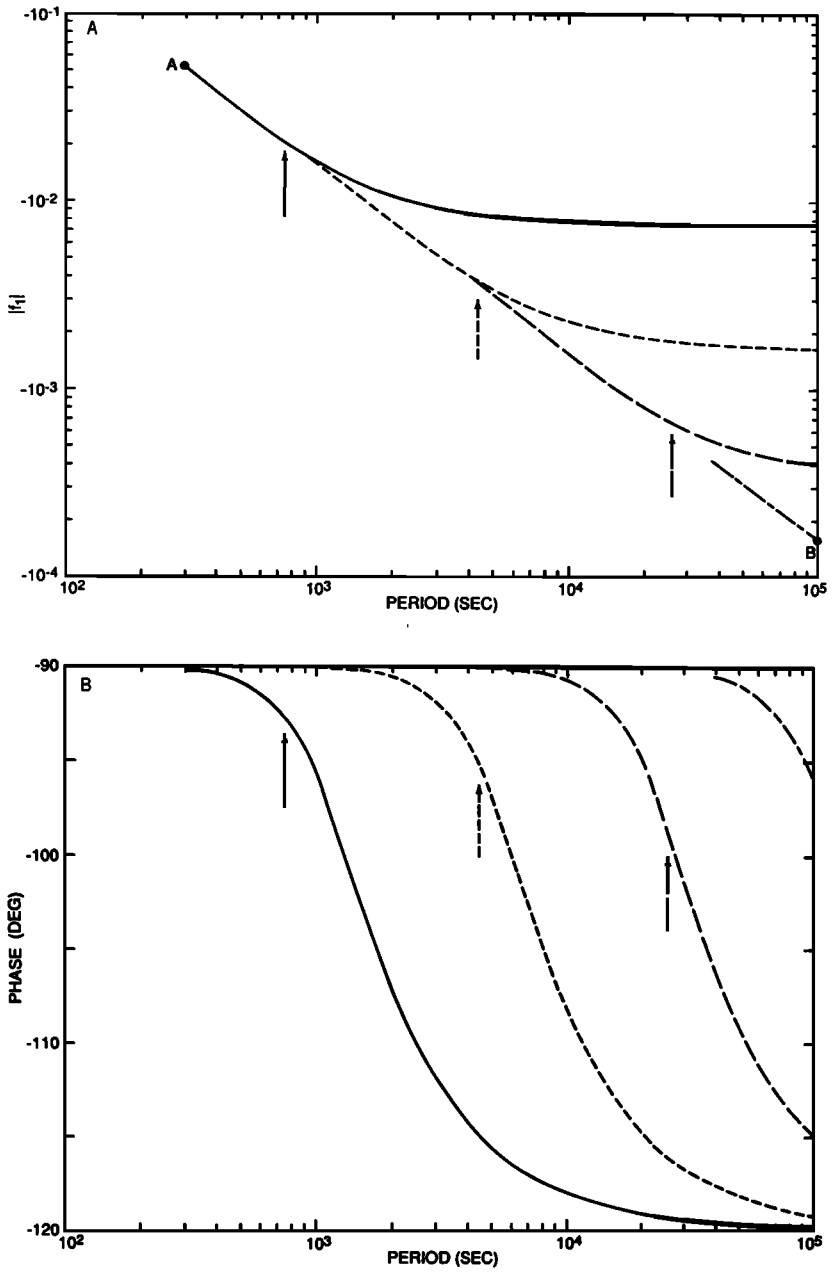

Fig. 2. (*a*) Magnitude and (*b*) phase of the dynamical factor f_1 versus period calculated with eddy dissipation and without Coriolis force. Curve styles correspond to the same wavelengths as in Figure 1, while the arrows show at what period for each particular wavelength the maximum amplitudes occur, as described in the text. Without dissipation both $|f_1|$ and the phase of f_1 would be independent of wavelength, with $|f_1|$ being represented as a straight line connecting the points labeled A and B in Figure 2*a* and with the phase of f_1 being equal to $-90°$.

regions of evanescence. Without dissipation included the values of $|\eta|$ for the 100- and 1000-km waves would be equal to $|\eta|$ for the 10-km wavelength wave at longer periods (i.e., the dashed and dashed-dotted curves would follow the solid curve at longer periods). The inclusion of dissipation, however, causes a departure from this situation at long periods, and the values of $|\eta|$ calculated with the inclusion of dissipation are significantly greater than their dissipationless counterparts, especially so for the shorter-wavelength waves. Once again, the arrows in this figure show the regions where the waves have reached their maximum amplitudes, as determined from Figure 1. One notices that for the 10- and 100-km wavelength waves the values of $|\eta|$ begin to depart significantly from their dissipationless values at periods where the wave amplitudes are beginning to decrease with increasing altitude (i.e., at periods to the right of the arrows), meaning that such modified values of $|\eta|$ are associated with waves which have achieved their maximum amplitudes at lower altitudes. However, a noticeable departure between the dissipationless value of $|\eta|$ and that calculated with the inclusion of dissipation has already occurred for the 1000-km wavelength wave at periods where maximum amplitudes are being achieved. This means that, all other assumptions aside, one should find it easier to observe values of $|\eta|$ which have been modified by dissipation for the longer-wavelength waves than for the shorter-wavelength waves.

The phase of η is shown in Figure 5*b*. For each value of horizontal wavelength it is shown both with and without the

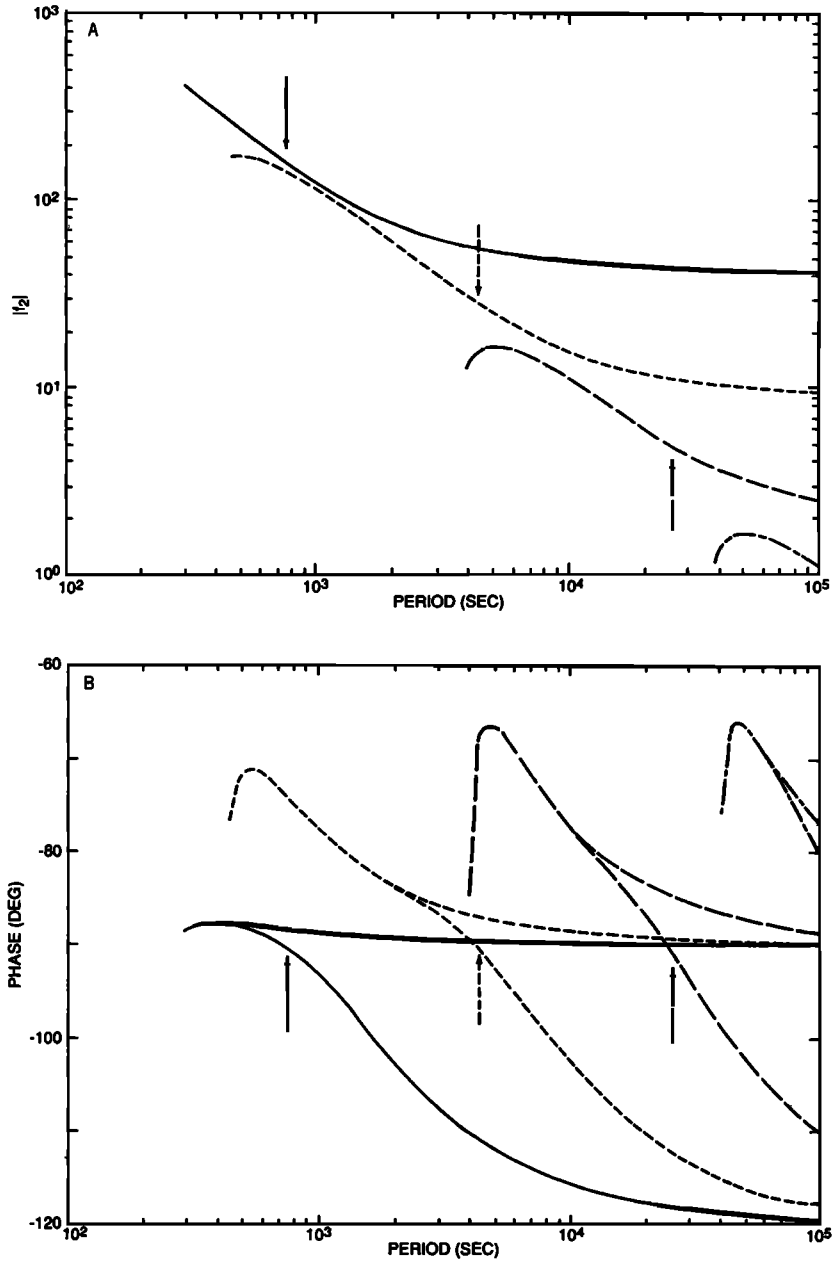

Fig. 3. As in Figure 2 but for the dynamical factor f_2. In the absence of any dissipation, $|f_2|$ would be independent of wavelength at long periods (see text for details). The upper and lower sets of curves in Figure 3*b* are those calculated without and with the inclusion of the eddy dissipation, respectively.

inclusion of dissipation. One notices that at long periods the phase of η calculated with the inclusion of dissipation is smaller than that calculated without dissipation, and that this effect is more pronounced for the shorter-wavelength waves. One also notices, in contrast to the results of $|\eta|$, that a departure between the dissipation and dissipationless phases of η begins before the waves have achieved a maximum amplitude for all wavelengths. This is especially so for the 10,000-km wavelength wave, which, though it never reaches a maximum amplitude for the periods considered nor has its values of $|\eta|$ modified very noticeably by the inclusion of dissipation, has its associated phase of η modified very noticeably by the inclusion of dissipation. For the other three wavelengths the differences between the phases of η calculated with the inclusion of dissipation and those calculated without it at periods where the waves are achieving maximum amplitudes are much larger for the longer-wavelength waves. Thus the phase of η appears to be more sensitive to the inclusion of dissipation than is $|\eta|$, while large modifications to the phase of η are more likely to be observed for the longer-wavelength waves which are achieving their maximum amplitudes.

Effect of Coriolis Force

In this section of results the effect of the Coriolis force is included in the gravity wave dynamics both with and without the effects of eddy dissipation included. Waves with horizontal wavelengths λ_x of 1000 and 10,000 km are studied. In order that the waves studied were internal gravity waves and not Rossby waves, the latitude used in all of the calculations was equal to 25°, giving an inertial period of slightly greater than 10^5 s. The results for this section are displayed only for the

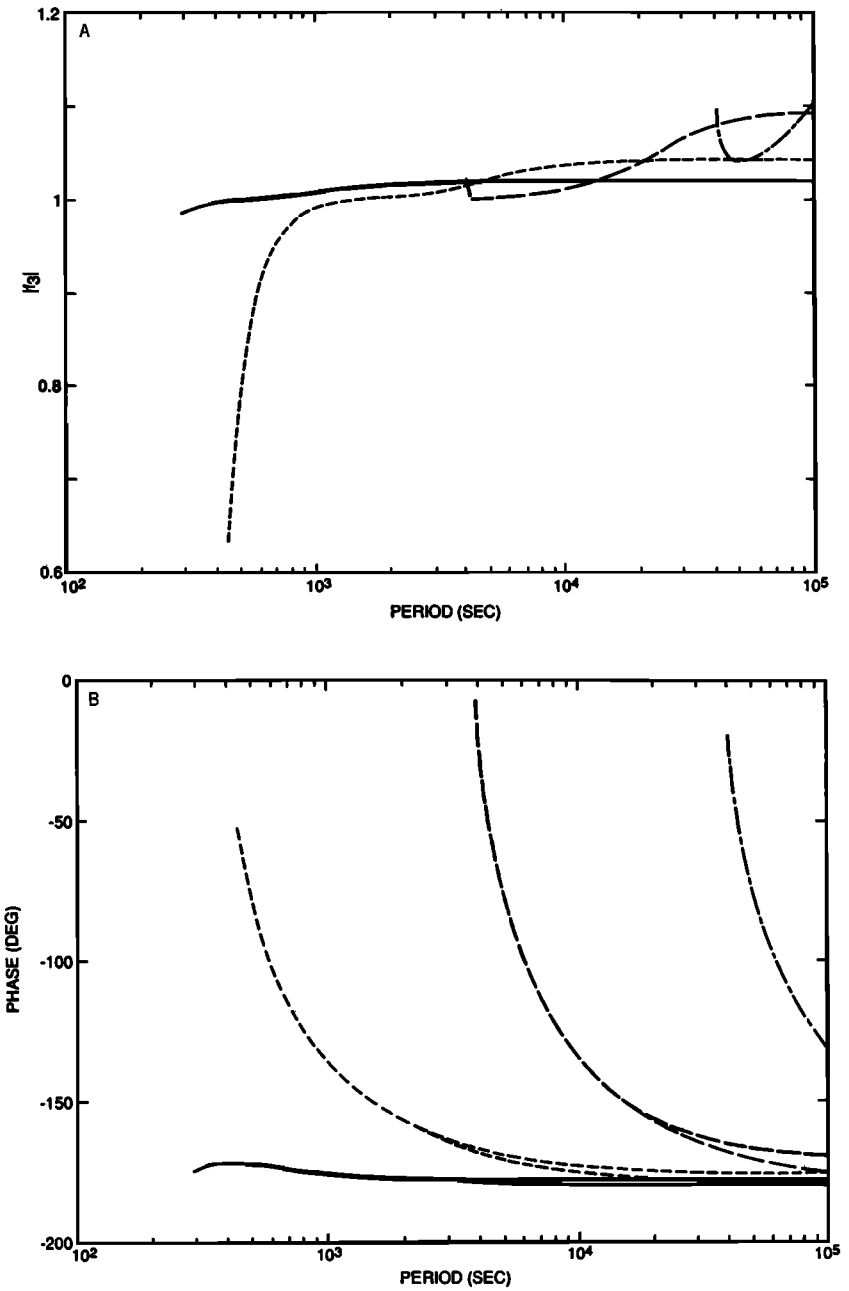

Fig. 4. As in Figure 3 but for the dynamical factor f_3. In the absence of any dissipation, $|f_3|$ approaches a wavelength-independent value of unity at long periods.

real and imaginary parts of the vertical wave numbers and for the magnitudes and phases of η.

Figure 6*a* shows the real part of the vertical wave number (Re (k_z)) as a function of wave period for $\lambda_x = 1000$ km. It can be seen that at the shorter wave periods the effects of eddy dissipation and Coriolis force on Re (k_z) are minimal. At the longer periods the effect of the Coriolis force is to increase the magnitude of Re(k_z) (i.e., decrease the vertical wavelength), while the effect of the eddy dissipation is to decrease the magnitude of Re (k_z) (i.e., increase the vertical wavelength). When the Coriolis force and the eddy dissipation are included together, the results at all wave periods are virtually the same as those resulting from the inclusion of the eddy dissipation alone, demonstrating the dominance of the eddy dissipation over the Coriolis force in the gravity wave dynamics for this particular value of horizontal wavelength.

The imaginary part of the vertical wave number (Im (k_z)) is shown in Figure 6*b*, along with the value of $1/2H$. Although by itself the Coriolis force is not responsible for any wave dissipation (so that Im (k_z) = 0), the value of Im (k_z) arising due to the eddy dissipation is, however, slightly modified by its further inclusion. The reasons for this will be explained shortly. Maximum wave amplitudes occur for periods close to about 23,000 s (6.4 hours).

The magnitude of η is shown in Figure 7*a*. By including only the Coriolis force, $|\eta|$ is increased by up to two orders of magnitude at long periods, but the further inclusion of the eddy dissipation reduces this quite markedly. The value of $|\eta|$ obtained with the inclusion of eddy dissipation alone is only slightly modified by the further inclusion of the Coriolis force, again demonstrating the dominance of the eddy dissipation over the Coriolis force for this particular value of horizontal

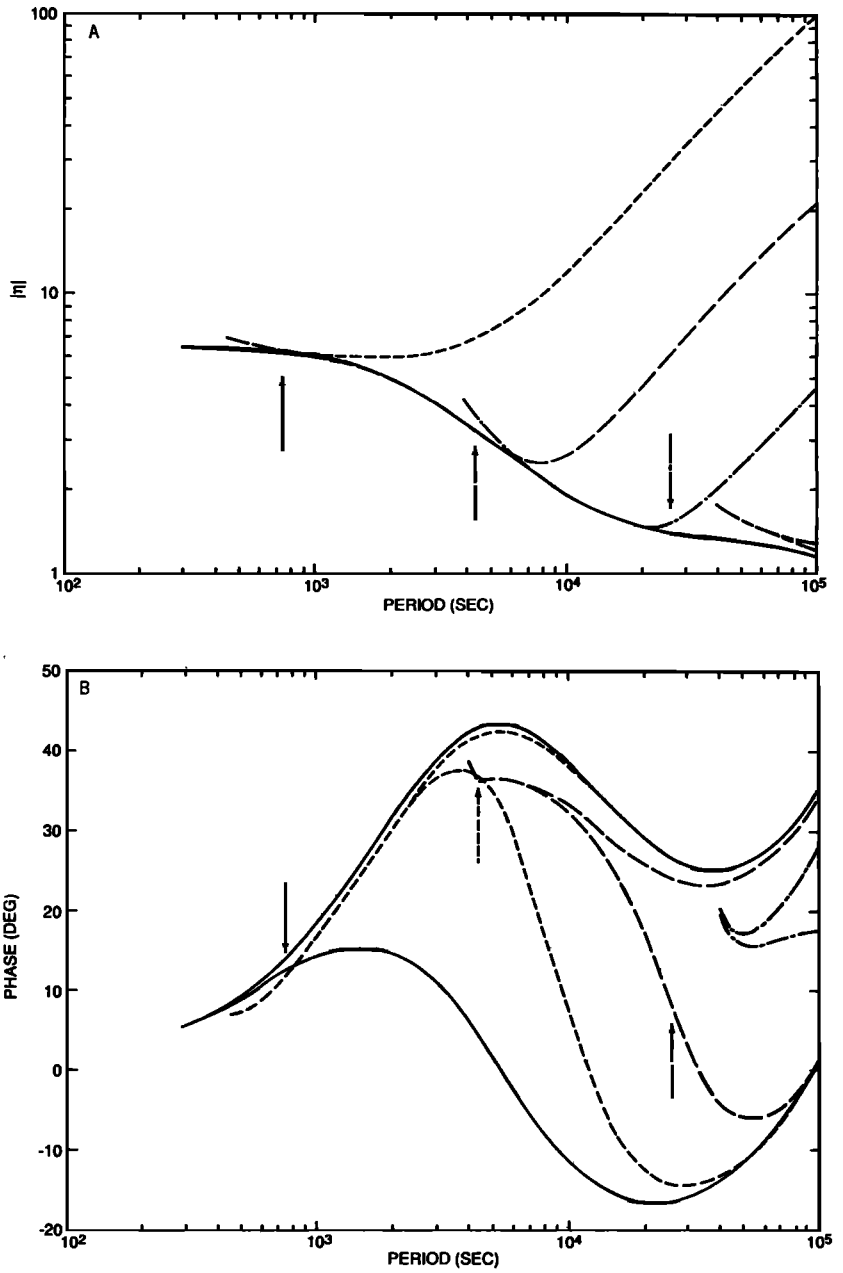

Fig. 5. (*a*) Magnitude and (*b*) phase of the ratio η of nightglow intensity fluctuations to temperature fluctuations versus period with eddy dissipation and without Coriolis force. In Figure 5*a*, horizontal wavelengths are 10 km (short-dashed curve), 100 km (long-dashed curve), 1000 km (dashed-dotted curve), and 10,000 km (short-and-long-dashed curve). The solid curve in Figure 5*a* is for a horizontal wavelength of 10 km but without eddy dissipation or Corilois force. In the absence of any dissipation all of the curves would follow the solid curve at long periods. In Figure 5*b*, horizontal wavelengths are 10 km (solid curves), 100 km (short-dashed curves), 1000 km (long-dashed curves), and 10,000 km (dashed-dotted curves). The lower and upper curves in Figure 5*b* are those calculated with and without the inclusion of the eddy dissipation, respectively.

wavelength. Hence the overall results obtained here for $|\eta|$ with both eddy dissipation and Coriolis force included are similar to those described in the previous results section.

The phase of η is shown in Figure 7*b*. Once again, although by itself the Coriolis force can cause significant modifications to the phase of η at long periods, it does not significantly modify the results obtained when it is included in conjunction with the eddy dissipation. As described in the previous results section, the phase of η is significantly modified at long periods by the inclusion of the eddy dissipation.

The real part of the vertical wave number (Re (k_z)) for λ_x = 10,000 km is shown in Figure 8*a*. One notices that Re (k_z) is modified only very slightly at long periods (and not at all at the shorter periods) by the inclusion of the eddy dissipation alone, while it is modified significantly at all periods, and more so at the longer periods, with the inclusion of the Coriolis force alone. With both eddy dissipation and Coriolis force included simultaneously, the modification to Re (k_z) at long periods is not as large as it is with the inclusion of the Coriolis force alone. The magnitude of Re (k_z) is increased (i.e., the vertical wavelength is decreased) at all periods by the simultaneous inclusion of the Coriolis force and the eddy dissipation,

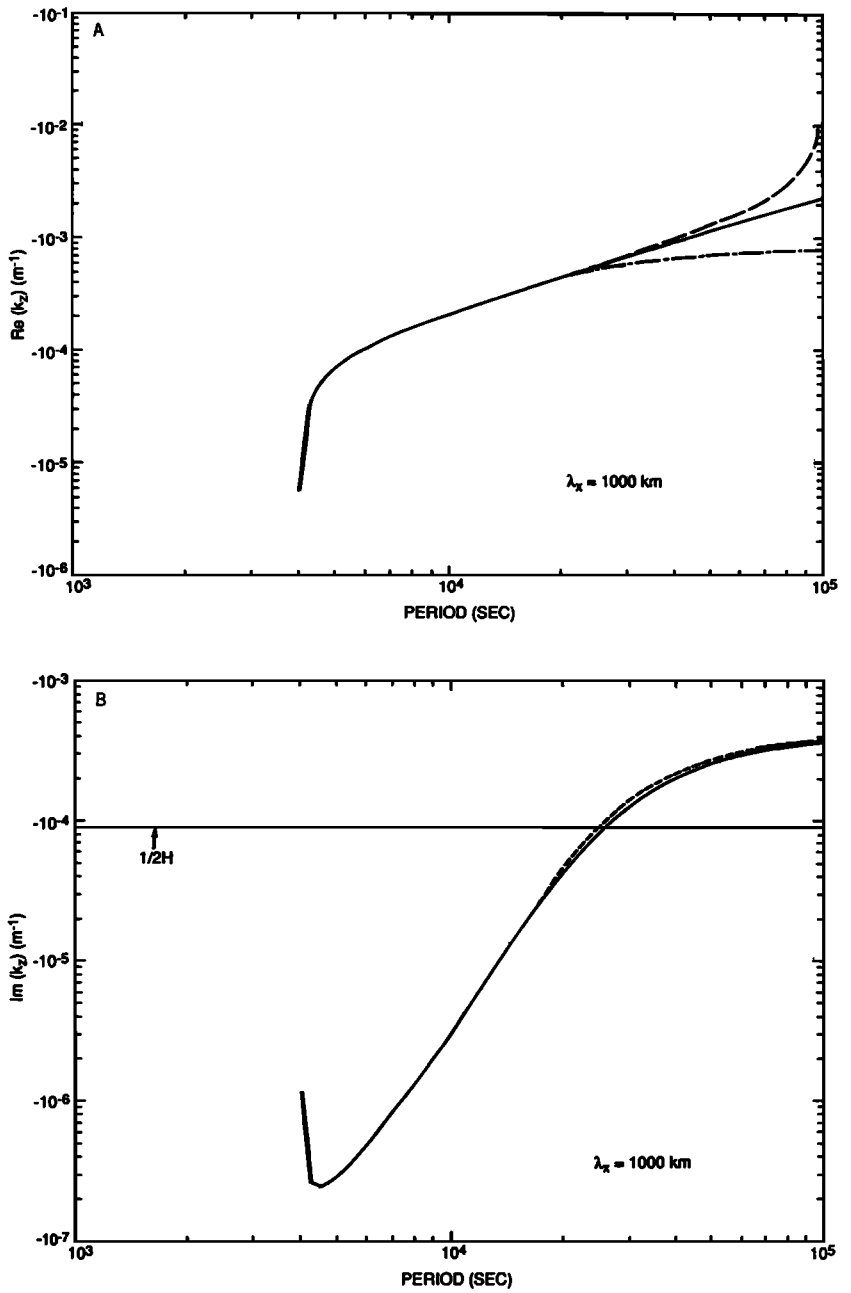

Fig. 6. (*a*) Real and (*b*) imaginary parts of the vertical wave number (k_z) versus period for a horizontal wavelength of 1000 km. The curves in Figure 6*a* are with no eddy dissipation or Coriolis force (solid curve), only Coriolis force (dashed curve), only eddy dissipation (dashed-dotted curve), or with both eddy dissipation and Coriolis force (dashed-dotted curve also). The curves in Figure 6*b* are with only eddy dissipation (solid curve) or with both eddy dissipation and Coriolis force (dashed curve). With only Coriolis force included, Im (k_z) = 0. The solid horizontal line shows the value of $1/2H$.

indicating the dominance of the Coriolis force over the eddy dissipation in the gravity wave dynamics for this particular value of horizontal wavelength.

The imaginary part of the vertical wave number (Im (k_z)) is shown in Figure 8*b*, along with the value of $1/2H$. With only eddy dissipation included, $|\text{Im}(k_z)|$ is much smaller than $1/2H$, demonstrating that there is very little wave dissipation at any wave period and that a maximum wave amplitude is never achieved. However, the further inclusion of the Coriolis force leads to an increased dissipation, and maximum wave amplitudes occur for periods close to 90,000 s (25 hours). The reason for this is that the effect of the further inclusion of the Coriolis force is to decrease the vertical wavelengths. Hence vertical velocity shears and vertical temperature gradients associated with the waves are increased, and so too are the viscous and thermal conduction dissipation rates.

The magnitude of η is shown in Figure 9*a*. The effect of including the Coriolis force alone is to increase $|\eta|$ several-fold at long periods, though the magnitude of this effect is substantially reduced by the further inclusion of the eddy dissipation. At the shorter wave periods the Coriolis force leads to a reduction in $|\eta|$ of several percent. While the eddy dissipation has little influence on $|\eta|$ at the shorter periods, at the longer periods its inclusion leads to an increase in $|\eta|$ of several per-

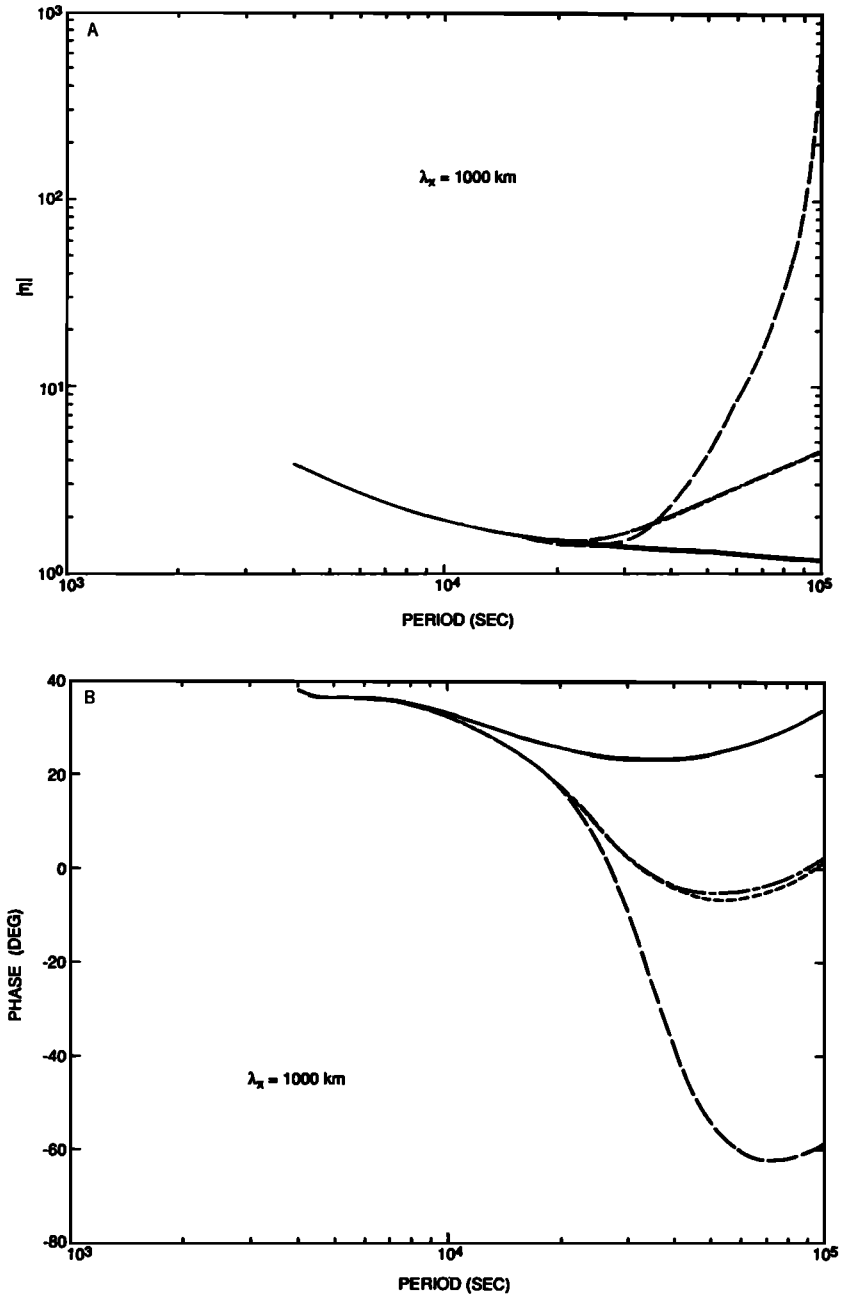

Fig. 7. (*a*) Magnitude and (*b*) phase of η versus period for a horizontal wavelength of 1000 km. The curves in Figure 7*a* are with no eddy dissipation or Coriolis force (solid curve) or with only Coriolis force (dashed curve). The remaining two curves in Figure 7*a*, which are difficult to distinguish, are with only eddy dissipation (small dashed, lower curve) or with both eddy dissipation and Coriolis force (dashed-dotted, upper curve). The curves in Figure 7*b* have similar meanings to those in Figure 7*a*, except that the long-and-short dashed curve represents results obtained with both eddy dissipation and Coriolis force.

cent. With the eddy dissipation and the Coriolis force included simultaneously, $|\eta|$ is decreased by several percent at the shorter periods and increased by some 25% at the longer periods.

The phase of η is shown in Figure 9*b*. By including the Coriolis force alone the phase of η is decreased by several degrees at the shorter periods, while at the longest of periods the amount of decrease is close to 80°. As in the case of $|\eta|$, however, the further inclusion of the eddy dissipation reduces the effect of the Coriolis force so that at the long periods the phase of η is decreased by only some 10° or so.

DISCUSSION

The results presented here have been performed assuming a Prandtl number of 2, but results to be presented elsewhere (NASA contract report, in preparation) have investigated the consequences of increasing the Prandtl number. As summarized in the discussion of *Hickey* [1988], while not affecting any of the main conclusions of that paper, the observability of some of the effects discussed there (and also here) may be diminished when the Prandtl number is increased. *Fritts and Dunkerton* [1985] have shown that turbulent Prandtl numbers

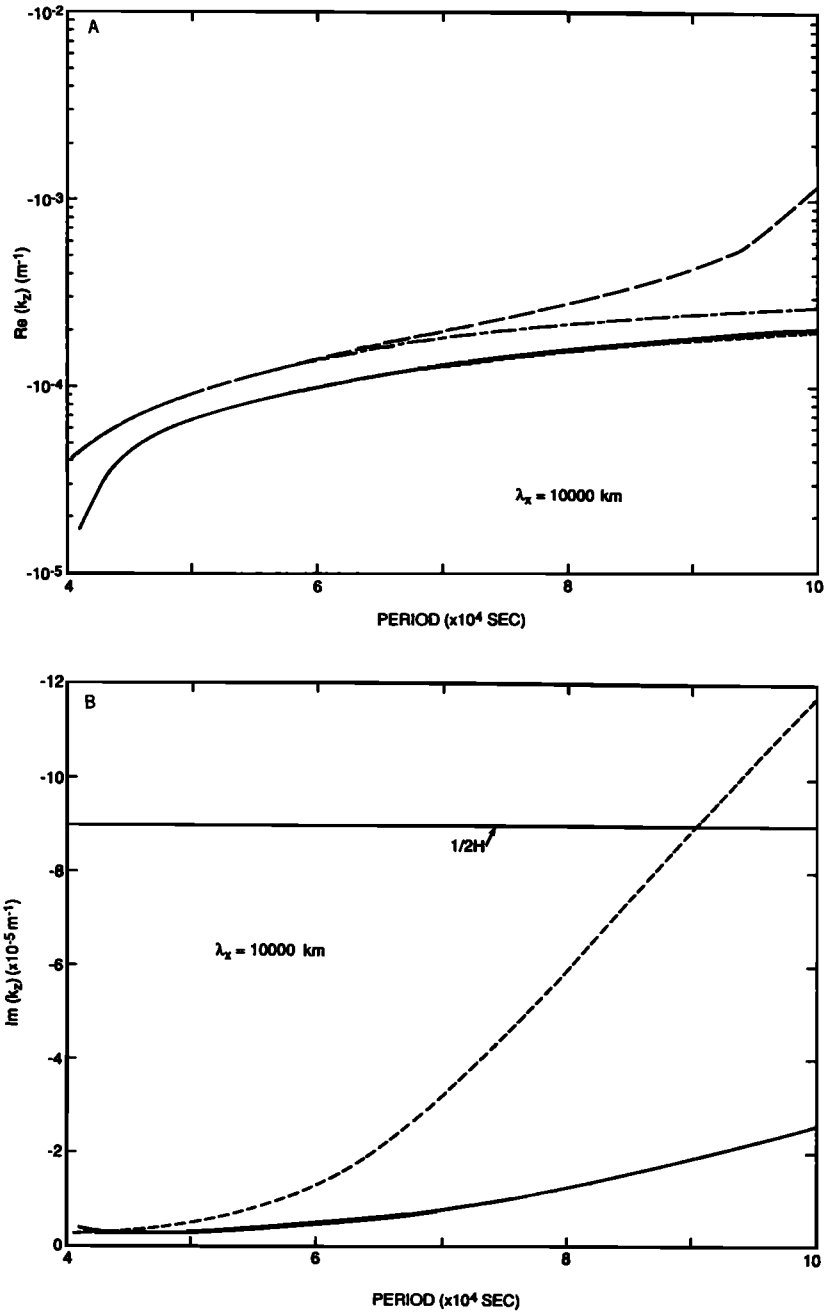

Fig. 8. (*a*) Real and (*b*) imaginary parts of the vertical wave number (k_z) versus period for a horizontal wavelength of 10,000 km. The curves in Figure 8*a* are with no eddy dissipation or Coriolis force (solid curve), only Coriolis force (long-dashed curve), only eddy dissipation (short-dashed curve), or with both eddy dissipation and Coriolis force (long-and-short-dashed curve). The curves in Figure 8*b* are with only eddy dissipation (solid curve) or with both eddy dissipation and Coriolis force (dashed curve). With only Coriolis force included, Im (k_z) = 0. The solid horizontal line shows the value of $1/2H$.

associated with convectively unstable gravity waves may achieve large values over limited regions of altitude within the mesosphere, suggesting that under such conditions it may be more difficult to measure values of η which have been noticeably modified by eddy dissipation.

In this study the maximum wave periods considered were 10^5 s ($\approx$27.8 hours), which is excessively high as far as realistic values of internal gravity wave periods are concerned. Nonetheless, in order that the waves studied not belong in the Rossby wave category, the latitude was taken to be 25° whenever the Coriolis force was included, giving an inertial period of some 28.3 hours. At higher latitudes the effect of the Coriolis force on η will be greater than that found here, though the maximum permissible internal gravity wave periods will be reduced. Even so, the results presented here demonstrate that the eddy dissipation dominates over the Coriolis force in the gravity wave dynamics for almost all of the wavelengths considered (the exception being the 10,000-km wavelength), so that the overall results and conclusions of this paper would not be substantially altered by changing the latitude.

For the 10,000-km wavelength the Coriolis force was found to be dominant in the gravity wave dynamics at the shorter

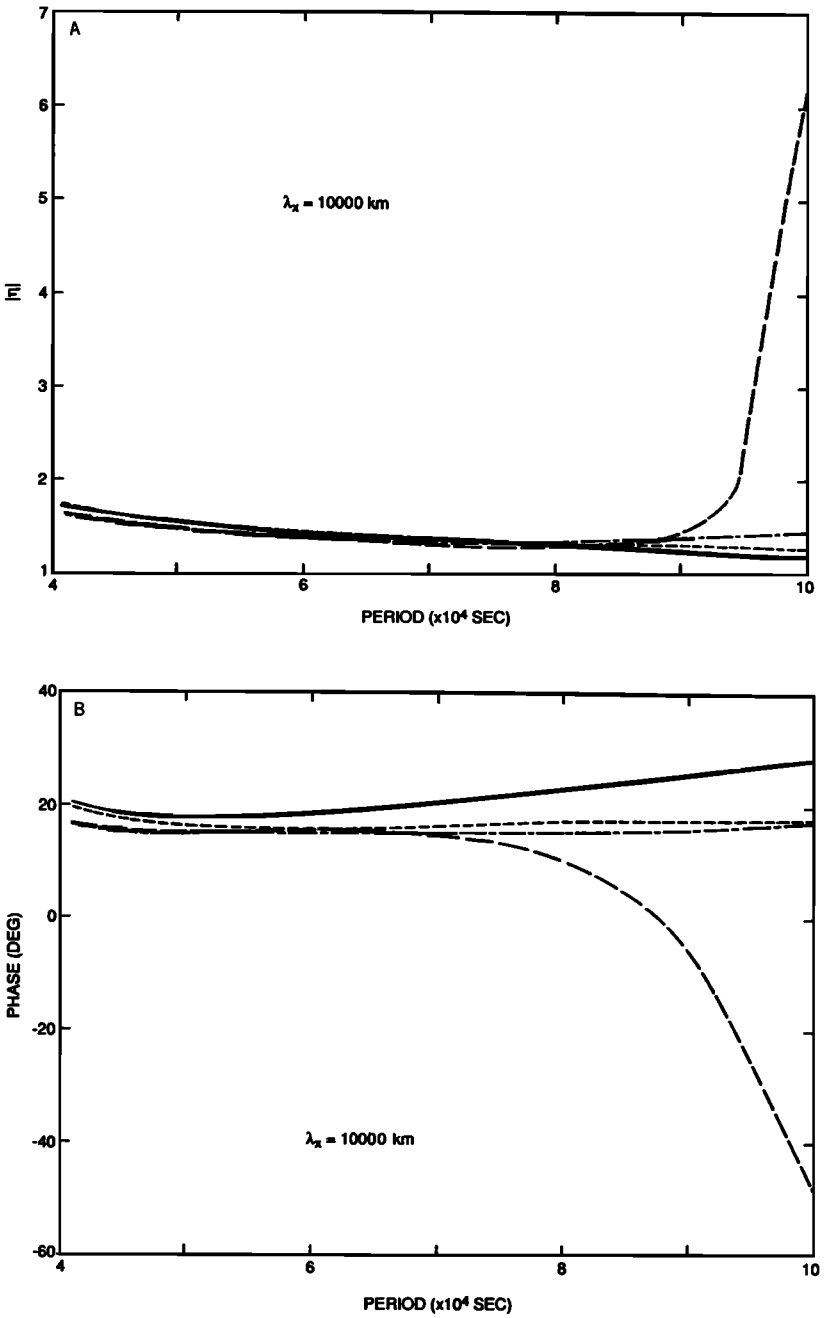

Fig. 9. (*a*) Magnitude and (*b*) phase of η versus period for a horizontal wavelength of 10,000 km with no eddy dissipation or Coriolis force (solid curves), only Coriolis force (long-dashed curves), only eddy dissipation (short-dashed curves), and both eddy dissipation and Coriolis force (long-and-short-dashed curves).

wave periods, as revealed by the modifications to η there, while it was found that at the longer periods the Coriolis force and eddy dissipation assumed equal importance. By itself the Coriolis force was found to cause large modifications to η at long wave periods, though this effect was reduced substantially by the further inclusion of the eddy dissipation. Although a full analysis is beyond the scope of the present work, these results suggest that some of the diurnal tidally driven fluctuations in the OH nightglow may be modified by eddy dissipation.

Also, all of the foregoing theory assumes the emission to occur at a single level in the atmosphere, whereas the emission layer is several kilometers thick. Thus interference between emissions from different levels will become important whenever the vertical wavelength is less than or comparable to the thickness of the emitting layer [*Hines and Tarasick*, 1987; G. Schubert and R. L. Walterscheid, Wave-driven fluctuations in OH nightglow from an extended source region, paper submitted to *Journal of Geophysical Research*, 1987]. This will introduce a further horizontal wavelength dependence on η which is not considered in the present analysis and which will be important for the shorter horizontal wavelength waves.

At the long wave periods, tidal contamination may modify some of the results presented here. Such contamination has been reported in the work by *Walterscheid et al.* [1986], in which a pseudotide was generated by gravity wave momentum fluxes modulated by the semidiurnal tide. The inclusion of such effects is beyond the scope of the present work.

CONCLUSION

The inclusion by *Hickey* [1988] of eddy dissipation and the Coriolis force in the gravity wave dynamics has placed a strong horizontal wavelength dependence on η which does not exist in the theory of *Walterscheid et al.* [1987]. Values of η have been found to depend on wave period and horizontal wavelength, so that internal gravity wave horizontal wavelengths will need to be measured in conjunction with the OH nightglow measurements if comparisons are to be made between observations and theory.

The eddy dissipation was found to dominate over the Coriolis force in the gravity wave dynamics and also in the associated values of η for the waves with horizontal wavelengths of 10, 100, and 1000 km, so that in these instances the Coriolis force can be neglected. The Coriolis force cannot be neglected for waves with horizontal wavelengths of 10,000 km or more, although the eddy dissipation, not as dominant as it is for the shorter wavelength waves, should also not be neglected.

At long periods the modifications to η by the inclusion of eddy dissipation are much larger for the shorter horizontal wavelength waves. Nonetheless, some of the longer horizontal wavelength waves may have associated with them values of η which have been more modified by its inclusion at periods where maximum amplitudes are being achieved. Thus, because there is an observational bias toward those waves achieving their maximum amplitudes, some of the more obvious modifications to η by the inclusion of eddy dissipation may be more observable for some of the longer horizontal wavelength waves.

The effect of eddy dissipation is to bring the OH intensity fluctuations more into phase with the temperature fluctuations (i.e., decrease the phase of η) and to increase the magnitude of the intensity fluctuation relative to the temperature fluctuation (i.e., increase $|\eta|$). The phase of η is more sensitive to the inclusion of eddy dissipation than is $|\eta|$ at periods where the eddy dissipation just begins to become important. When the Coriolis force becomes nonnegligible and is included with the eddy dissipation in the gravity wave dynamics, $|\eta|$ is decreased at the shorter wave periods and increased at long periods, while the phase of η is decreased at all periods.

APPENDIX

Assuming that the internal gravity waves are plane waves propagating in the x-z plane (x is horizontal coordinate; z is vertical coordinate), then one can write

$$\frac{\hat{n}}{n_0} = \frac{\hat{\rho}}{\rho_0}, \hat{\mathbf{v}}, \hat{T} \propto \exp i\,(\omega t - k_x x - k_z z - iz/2H) \quad \text{(A1)}$$

where n and ρ are the number and mass densities, respectively, a zero-subscripted variable refers to the undisturbed basic state, a circumflex denotes a wave variable, $\mathbf{v}$ is velocity, T is temperature, ω is the real wave angular frequency, k_x is the real horizontal wave number, k_z is the complex vertical wave number, and H is the scale height. The wave variables $\nabla \cdot \hat{\mathbf{v}}$, $\hat{w}$ (the vertical perturbation velocity), and $\hat{\rho}/\rho_0$ are related to $\hat{T}/T_0$ by the dynamical factors as follows:

$$\nabla \cdot \hat{\mathbf{v}} = f_1\, \hat{T}/T_0 \quad \text{(A2)}$$

$$\hat{w} = f_2\, \hat{T}/T_0 \quad \text{(A3)}$$

$$\hat{\rho}/\rho_0 = f_3\, \hat{T}/T_0 \quad \text{(A4)}$$

where

$$f_1 = i\omega\left\{\nu R - \frac{1}{(\gamma - 1)}\right\} \quad \text{(A5)}$$

$$f_2 = (\omega/k_x)\{x_1 + x_3[\nu R - (\gamma - 1)^{-1}]\} \quad \text{(A6)}$$

$$f_3 = \frac{\{i\alpha x_1 + x_2[\nu R - (\gamma - 1)^{-1}]\}}{(i\alpha x_3 - x_2)} \quad \text{(A7)}$$

and

$$x_1 = (i\alpha - \kappa)(\phi - c^2\phi^{-1}) + 3i\alpha\eta'$$

$$x_2 = -\eta'^2(\kappa - 3i\alpha)(\kappa + 2i\alpha) + [\eta'(4R - 1) - \beta'](\phi - c^2\phi^{-1} + \eta')$$

$$x_3 = \kappa(\phi - c^2\phi^{-1}) - 2i\alpha\eta' \quad \text{(A8)}$$

Also, following the notation of *Hickey and Cole* [1987],

$$\phi = 3\eta' R - \beta' \qquad R = \kappa^2 - i\alpha\kappa + 1$$

$$\kappa = \frac{k_z + \dfrac{i}{2H}}{k_x} \qquad \alpha = \frac{1}{k_x H}$$

$$\beta' = \frac{\omega^2}{gHk_x^2} \qquad \eta' = \frac{i\omega\mu}{3p_0} \quad \text{(A9)}$$

$$\nu = \frac{i\lambda T_0 k_x^2}{\omega p_0} \qquad c = \frac{f\omega}{gHk_x^2}$$

$$f = 2\Omega \sin\theta$$

Here, p_0 is the unperturbed pressure, g is the acceleration due to gravity, μ is the coefficient of (eddy) viscosity, λ is the coefficient of (eddy) thermal conduction, f is the Coriolis parameter, θ is the latitude, and $\Omega (= 7.29 \times 10^{-5}\ \mathrm{s}^{-1})$ is the Earth's angular frequency.

With viscosity, thermal conduction, and Coriolis force included, the vertical wave number is obtained from the quartic dispersion equation of *Hickey and Cole* [1987]. With only the Coriolis force included, the following dispersion equation is used:

$$k_z^2 = \frac{k_x^2(\omega_g^2 - \omega^2)}{(\omega^2 - f^2)} - \frac{(\omega_a^2 - \omega^2)}{C_s^2} \quad \text{(A10)}$$

where ω_g is the Brunt-Väisälä frequency ($=(\gamma - 1)^{1/2} g/C_s = 2.26 \times 10^{-2}\ \mathrm{s}^{-1}$), ω_a is the acoustic cutoff frequency ($= C_s/2H = 2.50 \times 10^{-2}\ \mathrm{s}^{-1}$), and C_s is the sound speed ($=(\gamma g H)^{1/2} = 274.8\ \mathrm{m\ s}^{-1}$).

Acknowledgments. I would like to thank my colleague S. A. Smith for many helpful discussions during the preparation of this paper. The paper has benefited from the comments of its reviewers. This work was supported by NASA contract NAS8-36400.

The Editor thanks C. S. Deehr and R. L. Walterscheid for their assistance in evaluating this paper.

REFERENCES

Fritts, D. C., and T. J. Dunkerton, Fluxes of heat and constituents due to convectively unstable gravity waves, *J. Atmos. Sci.*, *42*, 549–556, 1985.

Hecht, J. H., R. L. Walterscheid, G. G. Sivjee, A. B. Christensen, and J. B. Pranke, Observations of wave-driven fluctuations of OH nightglow emission from Sondre Stromfjord, Greenland, *J. Geophys. Res.*, *92*, 6091–6099, 1987.

Hickey, M. P., Effects of eddy viscosity and thermal conduction and

Coriolis force in the dynamics of gravity wave driven fluctuations in the OH nightglow, *J. Geophys. Res.*, this issue, 1988.

Hickey, M. P., and K. D. Cole, A quartic dispersion equation for internal gravity waves in the atmosphere, *J. Atmos. Terr. Phys.*, *49*, 889–899, 1987.

Hines, C. O., Internal atmospheric gravity waves at ionospheric heights, *Can. J. Phys.*, *38*, 1441–1481, 1960.

Hines, C. O., and D. W. Tarasick, On the detection and utilization of gravity waves in airglow studies, *Planet. Space Sci.*, *35*, 851–866, 1987.

Krassovsky, V. I., Infrasonic variations of OH emission in the upper atmosphere, *Ann. Geophys.*, *28*, 739–746, 1972.

Sivjee, G. G., R. L. Walterscheid, J. H. Hecht, R. M. Hamwey, G. Schubert, and A. B. Christensen, Effects of atmospheric disturbances on polar mesopause airglow OH emissions, *J. Geophys. Res.*, *92*, 7651–7656, 1987.

Walterscheid, R. L., G. G. Sivjee, G. Schubert, and R. M. Hamwey, Large-amplitude semidiurnal temperature variations in the polar mesopause: Evidence of a pseudotide, *Nature*, *324*, 347–349, 1986.

Walterscheid, R. L., G. Schubert, and J. M. Straus, A dynamical-chemical model of wave-driven fluctuations in the OH nightglow, *J. Geophys. Res.*, *92*, 1241–1254, 1987.

Winick, J. R., Photochemical processes in the mesosphere and lower thermosphere, in *Solar-Terrestrial Physics*, edited by R. L. Carovillano and J. M. Forbes, pp. 677–732, D. Reidel, Hingham, Mass., 1983.

M. P. Hickey, Universities Space Research Association, NASA Marshall Space Flight Center, ED-44, Huntsville, AL 35812.

(Received September 2, 1987;
revised December 10, 1987;
accepted January 15, 1988.)